

Nuclear dynamics in resonant electron-molecule scattering beyond the local approximation: Vibrational excitation and dissociative attachment in H₂ and D₂

Claus Mündel, Michael Berman,* and Wolfgang Domcke

Theoretische Chemie, Physikalisch-Chemisches Institut, Universität Heidelberg, im Neuenheimer Feld 253, D-6900 Heidelberg, West Germany

(Received 23 October 1984)

Vibrational excitation and dissociative electron attachment via the $^2\Sigma_u^+$ shape resonance in H₂ is treated within the framework of Feshbach's projection-operator formalism. The problem of nuclear motion in the complex, energy-dependent, and nonlocal potential of the $^2\Sigma_u^+$ resonance is solved with the use of a separable expansion of the nonlocal potential. The resonance energy, width function, and level-shift function, which characterize the resonance in the fixed-nuclei limit, are taken from recent *ab initio* calculations based on the many-body optical-potential approach [M. Berman, C. Mündel, and W. Domcke, Phys. Rev. A 31, 641 (1985)]. Integral cross sections for vibrational excitation of H₂ and D₂ up to $v=4$ and for dissociative electron attachment to H₂ and D₂ molecules in the vibrational levels $v=0, 1$, and 2 have been calculated. The calculations provide a good overall description of the experimental data for both H₂ and D₂. Pronounced isotope effects and a strong dependence of the attachment cross section on the vibrational state of the target molecule are found, in qualitative agreement with experimental observations. The accuracy of two widely used approximations, the adiabatic-nuclei approximation and the local-complex-potential model, is quantitatively assessed for this prototype resonance. While the off-shell adiabatic-nuclei approximation provides a qualitatively satisfactory description of vibrational excitation, we observe a stunning failure of the local-complex-potential model. Empirical local complex potentials, fitted to reproduce experimental vibrational excitation and dissociative attachment data in H₂ and D₂ within the local-potential model, lack any physical meaning.

I. INTRODUCTION

Since the pioneering work of Schulz and co-workers it is well established that resonances in electron-molecule scattering are a common phenomenon.¹ The most interesting and important aspect of electron-molecule-scattering resonances is the strong coupling of the electronic and nuclear motions. As a consequence, the cross sections for vibrational excitation of the target molecule are strongly enhanced in the energy range of a resonance.¹ Of particular interest are reactive processes such as dissociative attachment, where the short-lived collision complex decomposes into a stable negative ion and a neutral fragment.^{1,2} These inelastic and reactive collision processes constitute a major part of the physics and chemistry in outer space, in the higher atmosphere, and in discharges.³

The hydrogen molecule exhibits a broad low-energy shape resonance in electron scattering, leading to vibrational excitation and dissociative attachment in the (2–6)-eV energy range.^{4–6} Since H₂ is the simplest closed-shell molecular target, this resonance plays a prototypical role for our understanding of such collision processes. The first calculations of vibrational excitation and dissociative attachment in H₂ were performed by Bardsley, Herzenberg, and Mandl.^{7,8} They employed Siegert resonance theory to calculate the complex poles of the S matrix corresponding to the lowest $^2\Sigma_u^+$ and $^2\Sigma_g^+$ resonances in e -H₂ scattering.⁷ The resonance energy obtained in this way was adopted as a local complex poten-

tial energy for the nuclear motion to calculate the dynamical cross sections.⁸ The calculated resonance energies and widths were not accurate enough, however, to allow for a quantitative description of the experimental data.

Close-coupling calculations for rotational-vibrational excitation of H₂ were performed by Henry⁹ employing a static, model-exchange, and model-polarization potential for the e -H₂ interaction. Henry and Chang¹⁰ carried out an adiabatic-nuclei calculation of rotational-vibrational excitation cross sections. The first true *ab initio* study of vibrational excitation of H₂ was the calculation of Klonover and Kaldor¹¹ based on the adiabatic-nuclei approximation using T -matrix elements obtained with an L^2 basis-set method and a second-order many-body optical potential for the e -H₂ interaction. Very recently, Morrison and co-workers^{12,13} performed rotational and rotational-vibrational close-coupling calculations based on accurate fixed-nuclei scattering data and analyzed the accuracy of the adiabatic-nuclei approximation.

Several other treatments^{14–16} of rotational-vibrational excitation and dissociative attachment in H₂ were based on traditional resonant scattering theory, assuming a local complex potential for the nuclear motion in the resonance state as in Ref. 8. In these calculations the parameters characterizing the local complex potential were varied to achieve qualitative agreement with experimental vibrational excitation and/or dissociative attachment cross sections.^{14–16} As recently emphasized by Nesbet,¹⁷ the local complex $^2\Sigma_u^+$ potential-energy curves thus obtained differ

seriously from one another and from *ab initio* calculations.^{18,19} Indeed, the width of the ${}^2\Sigma_u^+$ shape resonance is so large at short internuclear distances that the applicability of the local-complex-potential model can reasonably be questioned. The local-complex-potential model has also been used in calculations of associative detachment in collisions of H^- with H .^{20,21} Bieniek²² has recently pointed out the possible breakdown of the local-complex-potential model for this process. Alternative models for dissociative attachment in H_2 and associative detachment in H^- - H collisions, which are based on Faddeev equations or a modified effective-range theory, have been proposed by Drukarev and Pozdnev²³ and by Gauyacq,²⁴ respectively.

In this work we present a unified treatment of vibrational excitation and dissociative electron attachment in H_2 using nonlocal Feshbach resonance theory as applied earlier to e - N_2 and e - F_2 scattering.^{25,26} While vibrationally elastic scattering and the excitation of low vibrational levels of H_2 seem to be very well understood theoretically,^{11-13,27,28} the present work represents the first *ab initio* calculation of the dissociative attachment cross section.

In the projection-operator approach²⁹ one introduces projectors

$$Q = |\psi_d\rangle\langle\psi_d|, \quad (1)$$

$$P = 1 - Q = \int dk k d\Omega_k |\hat{\psi}_k^{(\pm)}\rangle\langle\hat{\psi}_k^{(\pm)}| \quad (2)$$

in electronic Hilbert space, which are assumed to commute with the nuclear kinetic-energy operator T_N .³⁰⁻³⁴ In other words, the discrete state $|\psi_d\rangle$ and the background continuum states $|\hat{\psi}_k^{(\pm)}\rangle$ are diabatic^{35,36} electronic basis states. One obtains in this way a separation of the T matrix for electron scattering into a background term T_{bg} and a resonant term T_{res} . By construction, T_{bg} is a smoothly varying function of energy and generally weakly dependent on the internuclear distance R . The background scattering can thus be treated in the adiabatic-nuclei or impulse approximation.³⁷ The contribution of the resonant scattering to vibrational excitation and dissociative attachment, on the other hand, can be evaluated *exactly* by treating the nuclear dynamics in the short-lived negative-ion state, which is governed by an energy-dependent, complex, and nonlocal potential.^{25,26,30-34} The fixed-nuclei input data required in this approach are the potential energy $V_0(R)$ of the target molecule, the energy $\epsilon_d(R)$ of the discrete state $|\psi_d\rangle$, and the width and level-shift functions $\Gamma(R,E)$ and $\Delta(R,E)$.^{25,26} Methods for the *ab initio* calculation of these quantities have been developed by Hazi^{38,39} and by Berman and Domcke.⁴⁰ An alternative and largely equivalent formalism to treat vibrational excitation and dissociative attachment, which is based on the R -matrix approach, has been proposed by Schneider *et al.*⁴¹ and applied to the ${}^2\Pi_g$ shape resonance in N_2 .⁴²

The present work is based on *ab initio* calculated Feshbach resonance parameters $\epsilon_d(R)$, $\Gamma(R,E)$, and $\Delta(R,E)$ obtained recently by Berman, Mündel, and Domcke⁴³ (henceforth referred to as I). In these calculations the electron- H_2 interaction has been described in the many-body optical-potential formalism using the two-particle-

hole Tamm-Dancoff approximation (2ph-TDA).⁴⁴ The Schwinger variational principle^{45,46} has been used to solve the fixed-nuclei electron-molecule-scattering problem. Employing projection-operator techniques adapted to shape resonances,^{40,47} an explicit separation of the ${}^2\Sigma_u^+$ T matrix and eigenphase sum into a smooth background term and a rapidly varying (with respect to energy and internuclear distance) resonant term was achieved. To solve the difficult problem of nuclear motion in the energy-dependent, nonlocal, and complex potential of the ${}^2\Sigma_u^+$ resonance we avail ourselves of methods developed recently.⁴⁸ The local part $V_1(R) = V_0(R) + \epsilon_d(R)$ of the potential is represented by a Morse function and treated analytically, while the nonlocal part is approximated by a separable expansion⁴⁹ generated by the Lanczos basis of the Morse Hamiltonian.^{50,51}

Apart from obtaining reasonably accurate *ab initio* cross sections for vibrational excitation and dissociative attachment in H_2 and D_2 , our interest focuses on the analysis of the accuracy of two commonly employed approximations, namely the adiabatic-nuclei approximation and the local-complex-potential approximation. It will be seen that the ${}^2\Sigma_u^+$ shape resonance in H_2 provides a particularly clear-cut demonstration of the limitations of the local-complex-potential model for broad resonances.

II. THEORETICAL FRAMEWORK

A. The projection-operator formalism

The electronic projectors defined in Eqs. (1) and (2) define a separation of the *fixed-nuclei* elastic electron-molecule-scattering T matrix into a resonant and a background term according to

$$T(\mathbf{k}', \mathbf{k}) = T_{res}(\mathbf{k}', \mathbf{k}) + T_{bg}(\mathbf{k}', \mathbf{k}). \quad (3)$$

The resonant T matrix is given by the explicit expression^{29,40}

$$T_{res}(\mathbf{k}', \mathbf{k}) = V_{\mathbf{k}'}^{(-)} [k^2/2 - \epsilon_d - F(k)]^{-1} (V_{\mathbf{k}}^{+})^* \quad (4)$$

with the definitions

$$V_{\mathbf{k}}^{(\pm)} = \langle \hat{\psi}_{\mathbf{k}}^{(\pm)} | H | \psi_d \rangle, \quad (5)$$

$$\epsilon_d = \langle \psi_d | H | \psi_d \rangle, \quad (6)$$

$$F(k) = \langle \psi_d | H \hat{G}_{bg}^{(+)}(k) H | \psi_d \rangle. \quad (7)$$

Here $H = -\frac{1}{2}\nabla^2 + \Sigma$ is the effective electronic single-particle Hamiltonian which can be rigorously introduced via the many-body optical-potential approach.⁵² Σ is the energy-dependent and nonlocal self-energy of the one-body Green's function⁵³ and includes the static-exchange potential. A similar *ab initio* optical potential, which is based on the projection-operator formalism rather than the diagrammatic Green's-function approach, has recently been employed by Schneider and Collins.²⁷ The $|\hat{\psi}_{\mathbf{k}}^{(\pm)}\rangle$ are background scattering states defined as the solutions of the projected Lippmann-Schwinger equation^{40,47}

$$|\hat{\psi}_{\mathbf{k}}^{(\pm)}\rangle = |\mathbf{k}^{(\pm)}\rangle + \hat{G}_0^{(\pm)} \Sigma |\hat{\psi}_{\mathbf{k}}^{(\pm)}\rangle, \quad (8)$$

and $\hat{G}_{\text{bg}}^{(+)}$ in Eq. (7) is the corresponding Green's function. The $|\hat{\mathbf{k}}^{(\pm)}\rangle$ are plane-wave states, constrained to be orthogonal to the discrete state $|\psi_d\rangle$, and $\hat{G}_0^{(\pm)}$ is the associated free Green's function. Both can be constructed in closed form.^{47,54} A central quantity in the projection-operator formalism is the complex level-shift function of Eq. (7). It defines the width function $\Gamma(E)$ and the real level-shift function $\Delta(E)$ via

$$\Gamma(E) = -2 \text{Im}F(k), \quad (9)$$

$$\Delta(E) = \text{Re}F(k) \quad (10)$$

for real positive $k = \sqrt{2E}$. The level-shift $\Delta(E)$ for $E < 0$ is given by $F(k)$ with positive imaginary k .

When the nuclear degrees of freedom are included, the multichannel resonant T matrix can be written as a formal operator expression³³

$$T_{\text{res}}(\mathbf{k}_f, v'; \mathbf{k}_i, v) = (v' | V_{\mathbf{k}_f}^{(-)}(E - T_N - V_{\text{opt}})^{-1} (V_{\mathbf{k}_i}^{(+)})^* | v), \quad (11)$$

where \mathbf{k}_i and \mathbf{k}_f are the initial and final momenta of the scattered electron,

$$T_N = -(2\mu)^{-1} d^2/dR^2 \quad (12)$$

is the nuclear kinetic-energy operator, μ being the reduced mass, and

$$V_{\text{opt}} = V_1(R) + \Delta(R, E - \tilde{H}_0) - \frac{1}{2} i \Gamma(R, E - \tilde{H}_0) \quad (13)$$

with

$$V_1(R) = V_0(R) + \epsilon_d(R), \quad (14)$$

$$\tilde{H}_0 = T_N + V_0(R). \quad (15)$$

Here we have suppressed the rotational degrees of freedom, which is justified when considering vibrational excitation and dissociative attachment in low-temperature gases. The energy E in Eq. (11) is the total (electronic plus nuclear) energy

$$E = k_i^2/2 + \epsilon_v \quad (16)$$

which is conserved in the scattering process. The states $|v\rangle$ are vibrational eigenstates of the target molecule

$$\tilde{H}_0 |v\rangle = \epsilon_v |v\rangle. \quad (17)$$

We distinguish state vectors in the Hilbert space of nuclear motion from state vectors in the electronic Hilbert space by using rounded “|” and cornered “|” kets, respectively. $V_1(R)$ is the potential energy of the projected discrete state, while V_{opt} is the effective or “optical” potential which governs the nuclear motion in the resonance state. It is energy dependent, complex, and nonlocal.^{25,26,30–34} The nonlocality arises from the dependence of the width and level-shift operators on the nuclear kinetic-energy operator T_N contained in \tilde{H}_0 . Explicitly, the complicated operators $\Gamma(R, E - \tilde{H}_0)$ and $\Delta(R, E - \tilde{H}_0)$, which depend on the noncommuting operators R and \tilde{H}_0 , are defined as

$$\Gamma(R, E - \tilde{H}_0) = 2\pi \sum_m V_{E-\epsilon_m}(R) |m\rangle \langle m| V_{E-\epsilon_m}^*(R), \quad (18)$$

$$\Delta(R, E - \tilde{H}_0) = \sum_m P \int dE' \frac{V_{E'-\epsilon_m}(R) |m\rangle \langle m| V_{E'-\epsilon_m}^*(R)}{E - E'}, \quad (19)$$

where $V_E(R)$ is defined via

$$\Gamma(R, E) = 2\pi |V_E(R)|^2. \quad (20)$$

The summation over m in Eqs. (18) and (19) is meant to include integration over the continuous part of the spectrum of \tilde{H}_0 .

The operator expression (11) for the resonant electron-scattering T matrix including nuclear motion is essentially exact within the assumption of a diabatic discrete state and background continuum. The only additional approximation made in deriving Eqs. (11)–(15) (apart from the neglect of rotational motion, which could be straightforwardly included) is the assumption of a single electronic scattering channel, namely electronically elastic scattering.^{30–34} The coupling of the elastic channel with the infinite manifold of channels corresponding to excited electronic states, representing closed channels in low-energy electron-molecule scattering, has not been explicitly considered. In the present work the coupling to these closed channels is taken into account in the fixed-nuclei limit, using the many-body optical-potential approach. The channel coupling renders the fixed-nuclei electronic optical potential Σ and thus the effective electronic Hamiltonian H energy dependent. Therefore, ϵ_d defined in Eq. (6) is explicitly energy dependent and $F(k)$ in Eq. (7) acquires an additional energy dependence through H . In a complete non-Born-Oppenheimer theory the electronic optical potential Σ itself becomes a nonlocal operator in the *nuclear* coordinate R , in analogy to Γ and Δ discussed above. This nonlocality (with respect to the *nuclear* coordinate) of the polarization potential is not included in the present work. We treat the energy dependence of the polarization potential adiabatically by replacing $\epsilon_d(R, E)$ by $\epsilon_d(R) \equiv \epsilon_d(R, E_{\text{res}}(R))$, where $E_{\text{res}}(R)$ is the fixed-nuclei resonance energy defined by the implicit equation

$$E_{\text{res}}(R) = \epsilon_d(R, E_{\text{res}}(R)) + \Delta(R, E_{\text{res}}(R)). \quad (21)$$

For $e\text{-H}_2$ scattering this approximation is justified, since the energy dependence of ϵ_d is weak [see Fig. 6(a) in I]. Similarly, we neglect the weak additional polarization-induced energy dependence of Γ and Δ and make use of Eqs. (18) and (19), which, in a strict sense, are valid only in the absence of polarization effects.

By construction, the fixed-nuclei background T matrix T_{bg} introduced in Eq. (3) is weakly dependent on R and E in the energy region considered. The existence of such a separation of the fixed-nuclei T matrix into a smooth background term and a rapidly varying resonant term for the ${}^2\Sigma_u^+$ shape resonance in H_2 has been demonstrated in I. Therefore, the conditions required for the validity of the adiabatic-nuclei approximation³⁷ are fulfilled for the background scattering, and we may approximate the mul-

tichannel background T matrix as

$$T_{\text{bg}}(\mathbf{k}_f, v'; \mathbf{k}_i, v) = (v' | T_{\text{bg}}(\mathbf{k}_f, \mathbf{k}_i) | v), \quad (22)$$

where $T_{\text{bg}}(\mathbf{k}_f, \mathbf{k}_i)$ is the off-shell fixed-nuclei T matrix.^{55,56} In the present application the R dependence of $T_{\text{bg}}(\mathbf{k}_f, \mathbf{k}_i)$ is so weak⁴³ that the background contribution can be neglected for all but the vibrationally elastic channel. The formalism of Schneider *et al.*^{41,42} yields a similar separation of the multichannel R matrix into a "resonant" term and a "nonresonant" term, the latter being treated in the adiabatic-nuclei approximation.

Assuming that the dependence of the discrete-continuum coupling element $V_{\mathbf{k}}^{(\pm)}(R)$ on the angle $\Omega_{\mathbf{k}}$ does not change strongly with the internuclear distance, we can perform the angular integration and obtain for the integral resonant electron-molecule-scattering cross section^{57,58}

$$\sigma_{v'v}^{\text{res}}(E_i) = (4\pi^3 \nu / k_i^2) \times |(v' | V_{E_f}(E - T_N - V_{\text{opt}})^{-1} V_{E_i}^* | v)|^2, \quad (23)$$

where ν counts the spatial degeneracy of the discrete state ($\nu=1$ for the ${}^2\Sigma_u^+$ state of H_2^-).

The Feshbach formalism also yields a simple and formally exact (within the approximations discussed above) expression for the T -matrix element describing the rearrangement process of dissociative attachment^{31,58}

$$T_{\text{diss}}(K; \mathbf{k}_i, v) = (\tilde{K}^{(-)} | (V_{\mathbf{k}_i}^{(+)})^* | v), \quad (24)$$

where K is the asymptotic momentum in the dissociative channel and $|\tilde{K}^{(+)}$ is the scattering state describing nuclear motion in the nonlocal potential of the short-lived negative ion

$$|\tilde{K}^{(+)}\rangle = |K\rangle + G_0^{(+)} V_{\text{opt}} |\tilde{K}^{(+)}\rangle. \quad (25)$$

Here $|K\rangle$ is the plane-wave state describing free motion of the fragments and $G_0^{(+)} = (K^2/2\mu - T_N + i\eta)^{-1}$ is the corresponding free Green's function. The integral cross section for dissociative attachment reads [adopting energy normalization for the scattering states (25)]

$$\sigma_{\text{diss}}(E_i, v) = (4\pi^3 \nu / k_i^2) |(\tilde{K}^{(-)} | V_{E_i}^* | v)|^2. \quad (26)$$

Equation (26) is equivalent to expressions given in Refs. 26 and 57.

The widely used local-complex-potential model^{8,59} can be derived within the more general framework of the projection-operator approach.^{25,30-34} The local approximation consists in the replacement of the nonlocal operators $\Gamma(R, E - \tilde{H}_0)$ and $\Delta(R, E - \tilde{H}_0)$ defined in Eqs. (18) and (19) by the local functions

$$\Gamma(R) = \Gamma(R, E_{\text{res}}(R)), \quad (27a)$$

$$\Delta(R) = \Delta(R, E_{\text{res}}(R)), \quad (27b)$$

where $E_{\text{res}}(R)$ is the fixed-nuclei resonance energy defined in Eq. (21). With this approximation the optical potential for the nuclear motion becomes an energy-independent and local function of R

$$V_{\text{opt}}^L(R) = V_1(R) + \Delta(R) - \frac{1}{2}i\Gamma(R). \quad (28)$$

We have to replace, furthermore, the energy-dependent entrance and exit amplitudes V_{E_i} and V_{E_f} by local amplitudes, defined by (see, for example, Ref. 60)

$$W(R) = V_{E_{\text{res}}}(R) [E_{\text{res}}(R)]^{-1/4}. \quad (29)$$

The vibrational excitation and dissociative attachment cross sections in the local approximation are then given by Eqs. (23), (25), and (26) with V_{opt} and V_E replaced by the local quantities (28) and (29), respectively.

B. Parametrization of the fixed-nuclei data

The formalism outlined in the preceding subsection allows the calculation of vibrational excitation and dissociative attachment cross sections from a few input data which can be obtained by fixed-nuclei *ab initio* calculations. In detail, these quantities are (i) the potential-energy curve $V_0(R)$ of the target molecule, (ii) the energy $\epsilon_d(R)$ of the discrete state, defining the potential-energy curve of the discrete state according to $V_1(R) = V_0(R) + \epsilon_d(R)$, and (iii) the discrete-continuum coupling elements $V_E(R)$ which appear as entrance and exit amplitudes in Eqs. (23) and (26) and define the nonlocal width and level-shift functions according to Eqs. (18) and (19). These data are sufficient to evaluate the *resonant* electron scattering and dissociative attachment cross sections. If the background scattering contributes to vibrational excitation, the fixed-nuclei background T matrix $T_{\text{bg}}(\mathbf{k}', \mathbf{k})$ is also required as a function of R to evaluate the background contribution in the adiabatic-nuclei approximation.

In the present work, as in earlier calculations,^{25,48} we adopt the strategy of parametrizing the potential-energy curves $V_0(R)$, $V_1(R)$ and the coupling elements $V_E(R)$ by suitable analytic expressions so that most integrals required in the dynamical calculations can be performed analytically. The use of analytic parametrizations considerably reduces the number of (generally expensive) *ab initio* calculations required as a function of energy and internuclear distance. It allows us, moreover, to employ particularly efficient methods to deal with the nuclear dynamics in the nonlocal optical potential and thus to obtain numerically exact solutions for the model defined by the parametrization of the *ab initio* data.^{25,48}

For H_2 , a very accurate theoretical potential-energy function of the ${}^1\Sigma_g^+$ ground state is available.⁶¹ We have used a cubic-spline interpolation of these data to define $V_0(R)$.

The discrete-state energy $\epsilon_d(R, E)$ has been calculated in I for seven internuclear distances between $R=1.4014$ a.u. [the equilibrium geometry R_0 of H_2 (Ref. 62)] and $R=2.75$ a.u. The discrete-state energy is approximated here by the energy-independent quantity $\epsilon_d(R) = \epsilon_d(R, E_{\text{res}}(R))$, as explained above. $E_{\text{res}}(R)$ is the energy where the resonant ${}^2\Sigma_u^+$ eigenphase sum goes through $\pi/2$ (see I). To define $V_1(R)$ more accurately at short and large distances, the *ab initio* calculations of I have been augmented by calculations at two more internuclear distances, $R=1.0$ and 3.0 a.u. The *ab initio* data for $V_1(R) = V_0(R) + \epsilon_d(R)$ are interpolated and extrapolated by fitting a generalized Morse function⁶³

$$V_1(R) = D_1 \{ \exp[-2\alpha_1(R - R_1)] - 2t \exp[-\alpha_1(R - R_1)] \} + Q \quad (30)$$

to these data. $Q = 3.99$ eV is the known asymptotic limit of the ${}^2\Sigma_u^+$ state of H_2^- relative to the minimum of the ${}^1\Sigma_g^+$ state of H_2 . A good fit to the *ab initio* data is obtained with the following values of the parameters:

$$\begin{aligned} R_1 = R_0 = 1.4014 \text{ a.u.}, \quad t = 0, \\ D_1 = 1.7 \text{ eV}, \quad \alpha_1 = 1.19 \text{ a.u.}^{-1}. \end{aligned} \quad (31)$$

The potential-energy curve $V_1(R)$ of H_2^- is shown in Fig. 1(a) (chain curve) together with the *ab initio* values (stars)

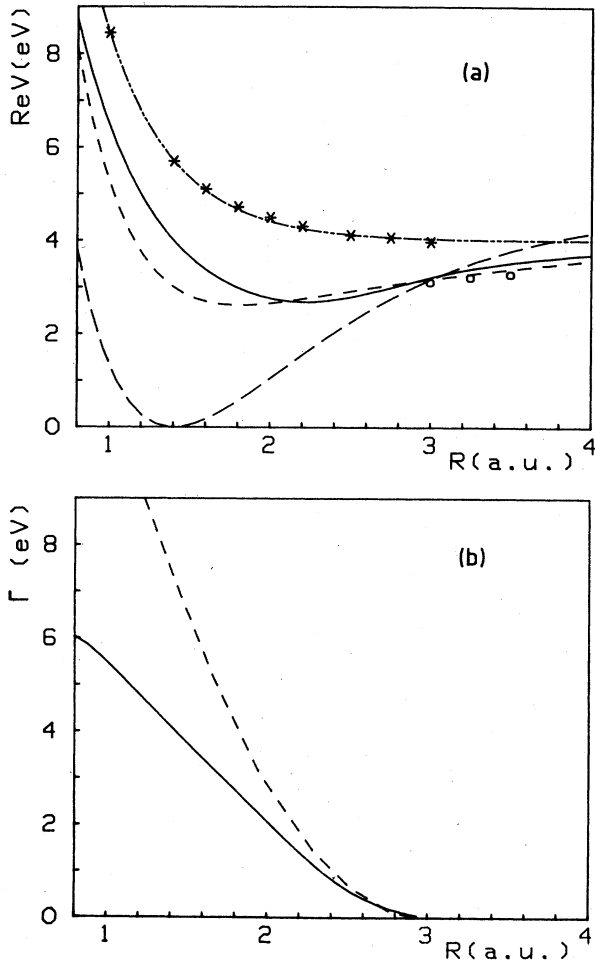


FIG. 1. Fixed-nuclei potential-energy curves for H_2 and H_2^- . The long-dashed curve in (a) gives the Kolos-Wolniewicz potential (Ref. 61) for the $X^1\Sigma_g^+$ ground state of H_2 . Stars give the *ab initio* calculated (Ref. 43) potential energy of the projected discrete ${}^2\Sigma_u^+$ state, the chain curve shows the analytic fit by the Morse function of Eq. (30) with the parameters of Eq. (31). The solid curve in (a) gives the real part of the local complex potential defined in Eq. (28). The corresponding local width function is shown in (b). The short-dashed curves show the empirical local complex potential determined by Bardsley and Wadehra (Ref. 16) (see text).

and the potential-energy curve $V_0(R)$ of H_2 (long-dashed curve). It is noteworthy that the discrete-state potential curve is purely repulsive.

In I the discrete-continuum coupling elements $V_k^{(+)}(R)$, the width function $\Gamma(R, E)$, and the level-shift function $\Delta(R, E)$ were obtained as a function of energy for a grid of seven internuclear distances. To fit these data by analytic functions we choose the *ansatz*

$$\Gamma(R, E) = 2\pi |V_E(R)|^2 = \left[\sum_{i=1}^3 f_i(E) g_i(R) \right]^2 \quad (32)$$

with

$$f_i(E) = A_i E^{3/4} e^{-B_i E}, \quad i = 1, 2, 3. \quad (33)$$

This *ansatz* incorporates the threshold law of Wigner⁶⁴ which requires $\Gamma(E) \sim E^{3/2}$ for a *p*-wave resonance. To fit the R dependence of the *ab initio* calculated $\Gamma(R, E)$, we tried both exponentials and Gaussians for the functions $g_i(R)$. The best fit was obtained with two Gaussians and one exponential, i.e.,

$$g_1(R) = e^{-C_1^2(R - R_0)^2}, \quad i = 1, 2 \quad (34a)$$

$$g_3(R) = e^{-C_3(R - R_0)} \quad (34b)$$

The fixed-nuclei level-shift function $\Delta(R, E)$ has been calculated in I for both positive and negative energies. To obtain a parametrization of $\Delta(R, E)$ which is suitable to evaluate the nonlocal level-shift operator $\Delta(R, E - \tilde{H}_0)$, we write Δ as the Hilbert transform of Γ ,

$$\begin{aligned} \Delta(R, E) &= \frac{1}{2\pi} \text{P} \int dE' \frac{\Gamma(R, E')}{E - E'} \\ &= \sum_{j=1}^6 G_j(R) \text{P} \int dE' \frac{F_j(E')}{E - E'}, \end{aligned} \quad (35)$$

neglecting thereby weak energy dependencies introduced by polarization effects.⁴⁰ The functions $F_j(E)$ and $G_j(R)$ follow trivially from Eqs. (32)–(34). The principal-part integral in Eq. (35) can be performed analytically.^{25,48}

With the parametrizations (32) and (35) we fitted simultaneously the *ab initio* data for $\Gamma(R, E)$ and $\Delta(R, E)$ by a nine-parameter least-squares fit. The resulting width and level-shift functions are shown in Fig. 2 (dashed curves) together with the *ab initio* result of I (solid curves). The values of the parameters A_i , B_i , and C_i , $i = 1, 2$, and 3 , are given in Table I. The agreement between the two sets of curves is satisfactory, especially for low energies and for internuclear distances near the equilibrium geometry of H_2 . The fit is less good at large internuclear distances, near the crossing point of the H_2 and H_2^- potentials. The

TABLE I. Coefficients for the width function $\Gamma(R, E)$ defined in Eqs. (32)–(34).

j	A_j (eV ^{-1/4})	B_j (eV ⁻¹)	C_j (a.u. ⁻¹)
1	0.7276	0.6932	0.0
2	0.5956	0.1711	0.3302
3	0.4583	0.0533	0.0489

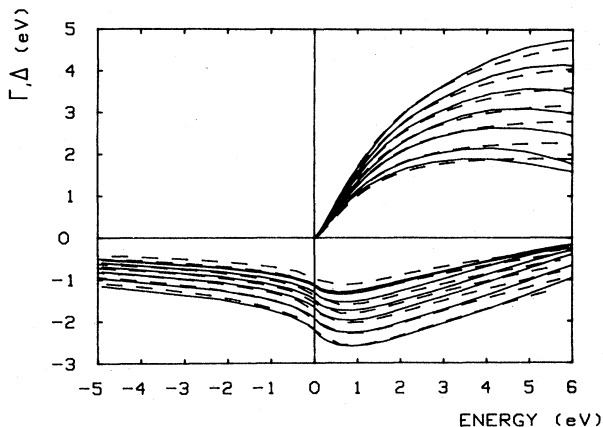


FIG. 2. *Ab initio* calculated width (upper curves) and level-shift (lower curves) functions as obtained in I (solid curve) as a function of energy and internuclear distance. The analytic fit provided by Eqs. (32)–(35) with the parameter values of Table I is shown by the dashed curves. The curves for the width Γ (level-shift Δ) correspond, from top to bottom (bottom to top), to the following internuclear distances (in a.u.): 1.4014, 1.6, 1.8, 2.0, 2.2, 2.5, and 2.75.

deviation seen in $\Gamma(E)$ for $E > 5$ eV should not affect the final results significantly, since the cross sections are peaked at lower energies (3–4 eV). The main features of the width and level-shift functions, namely the rapid increase of Γ with energy near threshold and the significant energy dependence of Δ around $E=0$, are accurately reproduced by the analytic fit. The fit determines, according to Eq. (32), also the discrete-continuum coupling elements $V_E(R)$ which appear as entrance and exit amplitudes in the cross-section formulas (23) and (26).

The real part of the local resonance potential energy, defined in Eq. (28), is included in Fig. 1(a) (solid curve). Since the level-shift Δ is large, the local resonance potential lies considerably below the potential curve $V_1(R)$ of the discrete state. It is interesting that the local resonance potential is attractive at large and intermediate distances, with a minimum near 2.2. a.u. and a well depth of more than 1 eV. The short-dashed curve in Fig. 1(a) is the real part of the empirical local resonance potential of Bardsley and Wadehra,¹⁶ to be discussed below. For completeness, the local width function $\Gamma(R)$ defined in Eq. (27a) is shown in Fig. 1(b) (solid curve) together with the empirical local width function of Ref. 16 (short-dashed curve). The local width increases monotonically with decreasing R , reaching a value of about 4 eV at the equilibrium geometry of H_2 .

The local ${}^2\Sigma_u^+$ resonance potential obtained in the present work crosses the ${}^1\Sigma_g^+$ ground state of H_2 at 3.03 a.u. Beyond that internuclear distance the ${}^2\Sigma_u^+$ state of H_2^- is bound. A presumably very accurate potential-energy function of the ${}^2\Sigma_u^+$ state in the range $3.0 \text{ a.u.} \leq R < \infty$ has recently been obtained by Senekowitsch *et al.*⁶⁵ using multireference configuration interaction techniques. These data are included as circles in Fig. 1(a). The calculations of Senekowitsch *et al.* show that the true

nonrelativistic Born-Oppenheimer ${}^2\Sigma_u^+$ potential of H_2^- is considerably more attractive at intermediate distances than previous *ab initio*⁶⁶ and empirical^{14,16,21} potentials, presumably owing to resonant electron exchange between H and H^- , which dominates over the polarization and van der Waals interactions⁶⁷ for $R \leq 10$ a.u. The present ${}^2\Sigma_u^+$ potential, being based on a Morse parametrization, does not take account of these subtle long-range effects and is seen to lie above the accurate potential of Ref. 65 for $R > 3$ a.u. This deficiency should not affect the vibrational excitation cross sections for low channels, but might affect the dissociative attachment cross section, which is peaked at the dissociation threshold.

C. Treatment of the nuclear dynamics

To solve for the nuclear scattering wave function in the nonlocal complex potential V_{opt} , we write Eq. (25) as

$$|\tilde{K}^{(+)}\rangle = |K^{(+)}\rangle + G_1^{(+)}F|\tilde{K}^{(+)}\rangle, \quad (36)$$

where

$$F = \Delta(R, E - \tilde{H}_0) - \frac{1}{2}i\Gamma(R, E - \tilde{H}_0) \quad (37)$$

is the nonlocal part of the potential, and $|K^{(+)}\rangle$ and $G_1^{(+)}$ are the scattering state and the Green's function for the local part $V_1(R)$. The scattering states ($R|K^{(+)}$) and Green's function $G_1^{(+)}(R, R')$ can be calculated analytically for the Morse potential (see, e.g., Ref. 63).

Approximating the nonlocal part F by the separable expansion⁴⁹

$$F^{(s)} = \sum_{i,j=1}^N F|\chi_i\rangle(B^{-1})_{ij}\langle\chi_j|F, \quad (38a)$$

$$B_{ij} = \langle\chi_i|F|\chi_j\rangle, \quad (38b)$$

the integral equation (36) reduces to a set of linear-algebraic equations and the corresponding T operator becomes⁴⁹

$$\tilde{T}^{(s)} = \sum_{i,j=1}^N F|\chi_i\rangle(A^{-1})_{ij}\langle\chi_j|F, \quad (39a)$$

$$A_{ij} = \langle\chi_i|(F - FG_1^{(+)}F)|\chi_j\rangle. \quad (39b)$$

The $\{(|R|\chi_i)\}$ are a set of square-integrable basis functions which will be specified below. In terms of the T operator $\tilde{T}^{(s)}$, the amplitudes for dissociative attachment and vibrational excitation are given by⁴⁸

$$\langle\tilde{K}^{(-)}|V_{E_i}^*|v\rangle = \langle K^{(-)}|(1 + \tilde{T}^{(s)}G_1^{(+)}V_{E_i}^*|v\rangle, \quad (40)$$

$$\begin{aligned} \langle v'|V_{E_f}(E - T_N - V_{\text{opt}})^{-1}V_{E_i}^*|v\rangle \\ = \langle v'|V_{E_f}G_1^{(+)}(1 + \tilde{T}^{(s)}G_1^{(+)}V_{E_i}^*|v\rangle. \end{aligned} \quad (41)$$

The integral cross sections are finally given by Eqs. (26) and (23), respectively.

The only approximation involved in these expressions is the truncation of the separable expansion (38) to a finite number of terms. Provided we can find a suitable set of basis functions ($R|\chi_i$) which renders the expansion (38) rapidly convergent, the truncation error can be made as

small as desired by including a sufficient number of terms. The obvious choice for the basis functions ($R | \chi_i$) would be the set of bound-state wave functions of the target Hamiltonian \tilde{H}_0 , since matrix elements of the nonlocal operator F are most conveniently evaluated in this basis [see Eqs. (18) and (19)]. A fundamental difficulty arises, however, from the incompleteness of the set of bound states of \tilde{H}_0 . Owing to this incompleteness, convergence of the results with the number N of basis functions is slow or even impossible. A suitable complete and orthonormal basis set is provided, however, by the Lanczos basis of the Morse Hamiltonian.^{48,50,51} The iteratively defined Lanczos basis functions⁵⁰ can be constructed explicitly for the Morse potential and read^{48,51}

$$\chi_n(z) = \left[\frac{\alpha n!}{\Gamma(2\gamma + n + 1)} \right]^{1/2} \times z^{\gamma+1/2} e^{-(1/2)z} L_n^{2\gamma}(z), \quad (42)$$

where

$$z = (2/\alpha)(2\mu D)^{1/2} \exp[-\alpha(R - R_0)] \quad (43)$$

and $\gamma > -\frac{1}{2}$, but otherwise arbitrary. The $L_n^\alpha(z)$ are generalized Laguerre polynomials.⁶⁸

In practice we introduce the Lanczos basis of $\tilde{H}_1 = T_N + V_1(R)$, the vibrational Hamiltonian of the discrete state. The tridiagonality of \tilde{H}_1 in the Lanczos representation leads to a simple three-term recursion relations for the matrix elements of $G_1^{(+)}$. All elements of $G_1^{(+)}$ can thus be obtained from the single element $\langle \chi_0 | G_1^{(+)} | \chi_0 \rangle$, which can be calculated analytically.⁴⁸ Selecting a large but finite set of Lanczos functions of \tilde{H}_1 , we diagonalize the target vibrational Hamiltonian \tilde{H}_0 in this basis. We thus obtain an approximate eigenbasis $\{(R | \bar{v})\}$ of \tilde{H}_0 which spans the space of bound states of \tilde{H}_0 and includes a discretized representation of the vibrational continuum. This approximate eigenbasis of \tilde{H}_0 is used to generate the separable expansion of F in Eq. (38) and to perform the internal sum over vibrational states in Eqs. (18) and (19). The contribution of the continuum of \tilde{H}_0 is thus included in both cases in a discretized manner. The introduction of the complete and orthonormal Lanczos basis is the essential step which allows us to obtain fully converged cross sections for vibrational excitation and dissociative attachment without recourse to the local approximation. More details can be found in Ref. 48.

The Lanczos basis functions contain the parameter γ which can be adjusted to optimize the convergence of the separable expansion (38). After a series of test calculations we have selected the values $\gamma=5$ for H_2 and $\gamma=10$ for D_2 . \tilde{H}_0 has been diagonalized in a basis of 60 Lanczos functions to generate the basis $\{(R | \bar{v})\}$. The matrix elements of the Kolos-Wolniewicz potential $V_0(R)$ with the Lanczos functions are calculated by numerical integration. The matrix elements of the kinetic-energy operator are given by simple analytic formulas.^{48,51} Converged results for the cross sections were obtained using 20 of these basis functions in the separable expansion of F . The matrix elements of $FG_1^{(+)}F$ entering Eq. (39b)

were calculated by inserting a basis between the operators F and $G_1^{(+)}$. Forty of the basis functions ($R | \bar{v}$) have been used for the insertion. The calculations based on the local approximation require a few more basis functions to achieve convergence. This emphasizes that the present method is especially adapted to the treatment of the nuclear dynamics in a nonlocal potential.

III. RESULTS

A. Comparison with experiment

We have calculated integral cross sections for vibrational excitation $v \rightarrow v'$ with $v=0$ and $v'=1, 2, 3$, and 4, as well as the cross section for dissociative electron attachment to molecules in the vibrational levels $v=0, 1$, and 2, considering both H_2 and D_2 . The vibrationally elastic electron-scattering cross section is given very accurately by the simple adiabatic-nuclei approximation (see Sec. IIIB) and thus does not require the application of the more elaborate nonlocal resonance theory. We have checked by adiabatic-nuclei calculations that the ${}^2\Sigma_u^+$ background T matrix in Eq. (3), owing to its weak dependence on R ,⁴³ contributes negligibly to vibrational excitation. It suffices, therefore, to evaluate the *resonant* vibrational excitation cross sections given by Eq. (23). We assume, furthermore, that the nonresonant symmetries ${}^2\Sigma_g^+$, ${}^2\Pi_g$, ${}^2\Pi_u$, etc., do not contribute to low-energy vibrational excitation and dissociative attachment in H_2 .

Figure 3 shows the calculated cross sections (solid curve) for the first four excitation channels $v'=1-4$ of H_2 in the (1-6)-eV energy range in comparison with the experimental data of Ehrhardt *et al.*^{4,69} (crosses). For the $0 \rightarrow 1$ excitation channel [Fig. 3(a)] the agreement between the present calculation and experiment is excellent, both for the energy dependence of the cross section as well as for its absolute magnitude. For the $0 \rightarrow 2$ channel [Fig. 3(b)] theory and experiment are still in agreement with respect to the absolute size of the cross section, but the

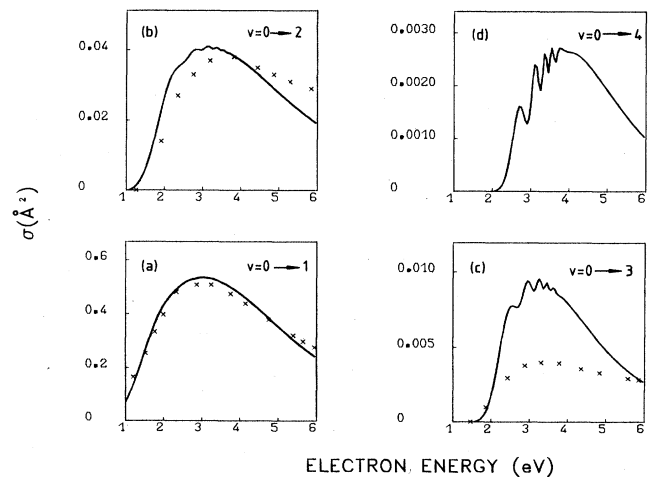


FIG. 3. Calculated and experimental integral vibrational excitation cross sections for electron- H_2 scattering. Solid curve is the result of the nonlocal resonance theory, crosses are the experimental data of Ehrhardt *et al.* (Refs. 4 and 69).

theoretical profile is peaked at lower energy and is narrower than found experimentally. For the $0 \rightarrow 3$ channel the theoretical cross section is larger than the experimental one by about a factor of 2 (note, however, the small absolute value of this cross section). No experimental data are available for the $0 \rightarrow 4$ vibrational excitation channel. Although the vertical energy of the ${}^2\Sigma_u^+$ resonance is close to 4 eV [see Fig. 1(a)], the $0 \rightarrow 1$ and $0 \rightarrow 2$ excitation functions are peaked at 3 eV. This shift results from the trivial prefactor k_i^{-2} in Eq. (23) as well as from nonlocal effects (see below). For higher inelastic channels the peak of the excitation function shifts to the right, being close to 4 eV for the $0 \rightarrow 4$ cross section.

The present integral $0 \rightarrow 1$ vibrational excitation cross section for H_2 is larger and in better agreement with the data of Ehrhardt *et al.*^{4,69} than the *ab initio* result of Klonover and Kaldor¹¹ obtained in the adiabatic-nuclei approximation using a second-order optical potential for the e - H_2 interaction. This finding is consistent with the trends observed in the fixed-nuclei limit. As shown in I, the more sophisticated 2ph-TDA optical potential yields a ${}^2\Sigma_u^+$ eigenphase sum and cross section that are larger than the second-order result. The present results for the $0 \rightarrow 1$ vibrational excitation channel of H_2 are also in good agreement with *ab initio* rotational-vibrational close-coupling calculations by Morrison and co-workers.¹³

An interesting and somewhat unexpected feature of the present results for H_2 is the appearance of fine structure in the excitation functions for $v \geq 3$. This fine structure is associated with short-lived vibrational levels of H_2^- which converge to the dissociation limit at 3.725 eV. So far the ${}^2\Sigma_u^+$ shape resonance in H_2 has been considered the prototype example of an extremely short-lived resonance where the nuclear motion can be described in the impulse limit.^{8,70} The appearance of fine structure can be qualitatively rationalized, however, by considering the local complex potential energy of H_2^- shown in Fig. 1. The real part of the local resonance potential exhibits an attractive well which is deep enough to support many vibrational levels. The local width $\Gamma(R)$, though very large at the equilibrium geometry of H_2 , decreases quickly with increasing internuclear distance [see Fig. 1(b)]. It follows from the strongly anharmonic shape of the real part of the local potential that the nuclei will spend most of the time in the outer region, where $\Gamma(R)$ is small or even zero. As a consequence, the autoionization probability is strongly quenched. The importance of this "vibration-induced narrowing effect" has been emphasized previously.⁷¹ The details of the fine structure depend very sensitively on the energy and width of the resonance over a wide range of internuclear distances. They represent, therefore, a stringent test for the accuracy of the *ab initio* calculation. The fine structure cannot be reproduced by calculations based on the adiabatic-nuclei approximation and is possibly difficult to obtain by close-coupling calculations, owing to slow convergence, as found before for the substructure of the ${}^2\Pi_g$ resonance in N_2 .⁷²

Figure 4 shows the calculated vibrational excitation cross sections for D_2 . These cross sections are smaller than the corresponding cross sections in H_2 and decrease faster with increasing v' . This result is in agreement with

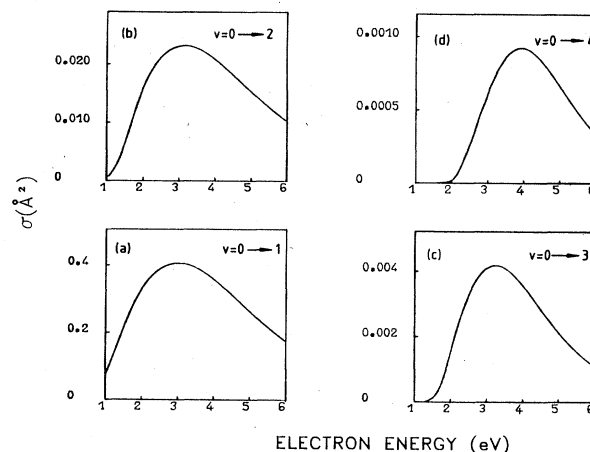


FIG. 4. Calculated integral vibrational excitation cross sections for electron- D_2 scattering.

the qualitative picture that the nuclear motion in D_2 is more sluggish than in H_2 and thus cannot pick up the same amount of momentum during the short lifetime of the resonance. The ratio of the peak values of the calculated integral $0 \rightarrow 1$ cross sections for D_2 and H_2 is about 0.7, in agreement with earlier theoretical predictions.⁷³ The only experimental information we are aware of is a measured ratio of 0.75 (0.55) for rotationally resolved $\Delta_j = 2$ ($\Delta_j = 0$) transitions at 4-eV impact energy and 90° scattering angle.⁷³ As in H_2 , we observe that the excitation functions peak at higher energy and become narrower with increasing v' . Also noteworthy is the complete absence of vibrational fine structure even for the $0 \rightarrow 4$ channel, in marked contrast to the results for H_2 . This difference is a consequence of the slower vibrational motion of D_2 , which implies that the vibrational-narrowing effect is less efficient in D_2 than in H_2 .

The calculated integral cross sections for dissociative electron attachment to H_2 and D_2 in their vibrational ground states are shown in Fig. 5. The experimental data of Schulz and Asundi⁶ are included as crosses. The calculation reproduces the expected nearly vertical onset of the cross sections at the threshold and their rapid decrease at higher energies, although the theoretical profiles are somewhat broader than the observed ones. The peak values of the calculated cross sections are about 50% larger than the experimental peak values for both H_2 and D_2 . Considering the very small absolute magnitude of the dissociative attachment cross sections and their sensitivity to details of the *ab initio* nonlocal resonance potential, this kind of agreement is rather satisfactory.

Since the nuclei in H_2 move faster, they have a higher probability of dissociating before the short-lived ${}^2\Sigma_u^+$ resonance decays. Therefore, the dissociative attachment cross section is much larger in H_2 than in D_2 . The calculated ratio of the peak values of the dissociative attachment cross sections for H_2 and D_2 is 200, in excellent agreement with the measured value of $200 \pm 20\%$.⁶

Allan and Wong⁷⁴ have measured dissociative attachment in H_2 and D_2 at temperatures ranging from 300 to 1600 K and have extracted cross sections for attachment

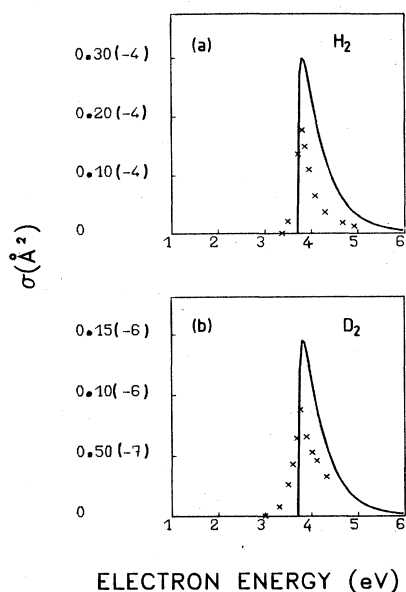


FIG. 5. Calculated and experimental integral cross sections for dissociative attachment in H_2 (a) and D_2 (b). Solid curve is the result of the nonlocal resonance theory, crosses are the experimental data of Schulz and Asundi (Ref. 6).

to rotationally and vibrationally excited molecules. A dramatic increase of the attachment cross section with increasing vibrational excitation of the target was observed.⁷⁴ The present results for dissociative attachment to H_2 in the initial states $v=0, 1$, and 2 are shown in Fig. 6. To facilitate the display, the $v=1$ cross section has been scaled down by a factor of 0.1 , the $v=2$ cross section by a factor of 0.01 . It is seen that the shape of the cross sections changes little with v . The calculated attachment cross sections exhibit the expected increase with v , but this increase is less pronounced than found experimentally.⁷⁴ Table II summarizes the calculated and observed peak values of the cross section for dissociative attachment to H_2 and D_2 in the initial states $v=0, 1$, and 2 .

B. Accuracy of the adiabatic-nuclei and local-complex-potential approximations

To the extent that the discrete state $|\psi_d\rangle$ is diabatic and the contribution of the background negligible for inelastic and reactive processes, the results presented in the

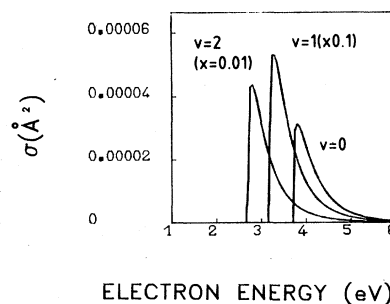


FIG. 6. Calculated cross sections for dissociative attachment of electrons to H_2 in the initial vibrational level $v=0, 1$, and 2 . For the purpose of display, the $v=1$ cross section has been reduced by a factor of 0.1 , the $v=2$ cross section by a factor of 0.01 .

preceding subsection are based on an exact treatment of the vibrational and dissociative dynamics beyond the Born-Oppenheimer approximation. The nonlocal Feshbach resonance theory requires, however, a considerable computational effort to generate the *ab initio* input data $\epsilon_d(R)$, $\Gamma(R,E)$, $\Delta(R,E)$ and to solve for the nuclear dynamics in the nonlocal complex potential. For this reason the theory has so far been applied only to the simplest electron-molecule-collision systems, namely $e\text{-N}_2$,²⁵ $e\text{-F}_2$,²⁶ and $e\text{-H}_2$ (this work). The same applies to the *ab initio* multichannel R -matrix theory, which has so far been applied only to vibrational excitation of N_2 .⁴² To treat the collision of electrons with polyatomic targets, one has to resort to computationally simpler methods based on more crude approximations. It is certainly desirable to test the accuracy of these approximate methods in cases where more accurate treatments are possible, such as in the present case.

The simplest and most widely used approximation to describe vibrational excitation by electron impact is the adiabatic-nuclei approximation.^{37,55,75} In the context of resonant electron-molecule scattering this approximation is expected to be applicable for short-lived resonances.⁷⁰ It is bound to fail for long-lived resonances since it cannot reproduce the substructure of the cross sections associated with the vibrational motion of the negative ion.⁷⁰ In its simplest version the adiabatic-nuclei approximation for vibrational excitation involves vibrational matrix elements of the on-shell fixed-nuclei T matrix.^{55,75} In the present case we are in the position to employ a more sophisticated version which involves an approximate off-shell fixed-

TABLE II. Peak values of the integral dissociative attachment cross section (in \AA^2) for H_2 and D_2 in the vibrational states $v=0, 1$, and 2 . Digits in parentheses indicate powers of ten.

v	H_2			D_2		
	Theor. ^a	Expt. ^b	Local ^c	Theor. ^a	Expt. ^b	Local ^c
0	3.0(-5)	1.6(-5)	2.8(-4)	1.5(-7)	8.0(-8)	3.2(-6)
1	5.2(-4)	5.5(-4)	2.7(-3)	3.5(-6)	3.6(-6)	4.0(-5)
2	4.3(-3)	8.0(-3)	1.5(-2)	4.3(-5)	9.0(-5)	2.9(-4)

^aNonlocal resonance theory, this work.

^bReferences 6 and 74.

^cLocal-complex-potential approximation, this work.

nuclei T matrix. We have evaluated the resonant T matrix of Eq. (11) in the adiabatic-nuclei approximation using the appropriate off-shell amplitudes V_{E_i} and V_{E_f} and replacing E in the denominator by the geometric mean $(E_i E_f)^{1/2}$.

The second widely employed model to rationalize the nuclear dynamics in resonant electron-molecule scattering is the local-complex-potential approximation.^{8,59,70} In this approximation the energy-dependent and nonlocal operator $V_{\text{opt}}(R, E - \hat{H}_0)$ given by Eqs. (13), (18), and (19) is replaced by the energy-independent and local function $V_{\text{opt}}^L(R)$ as explained in Sec. II A. The local approximation is expected to fail for resonances near threshold^{22,32} and for very broad resonances, as confirmed recently by numerical calculations for certain simple models.^{60,76} The local-complex-potential model is thus to some extent complementary to the adiabatic-nuclei approximation. In contrast to the latter, the local-complex-potential model also permits the calculation of dissociative attachment cross sections.

Figure 7 shows vibrational excitation functions for $v=0 \rightarrow 1, 2$, and 3 and the dissociative attachment cross section in H_2 calculated in the adiabatic-nuclei approximation and the local-complex-potential approximation in comparison with the results of the nonlocal Feshbach resonance theory. We discuss the adiabatic-nuclei results first. For the resonant vibrationally elastic cross section (not shown) the standard as well as the off-shell adiabatic-nuclei result is indistinguishable from the nonlo-

cal Feshbach result. This proves that the adiabatic-nuclei approximation is sufficient to calculate the vibrationally elastic cross section; the separation of the fixed-nuclei $^2\Sigma_u^+$ T matrix into a resonant and a background contribution is thus unnecessary for this channel. For the inelastic channels the standard on-shell adiabatic-nuclei theory is less satisfactory than the off-shell version, particularly so for large $|v'-v|$, as expected. The results of the off-shell adiabatic-nuclei theory are displayed in Figs. 7(a)–7(c). This approximation is of excellent accuracy for the $v=0 \rightarrow 1$ channel; the accuracy deteriorates for the higher channels where the exact cross sections start to develop fine structure. Nevertheless, the overall magnitude of the cross sections is reliably predicted by the off-shell adiabatic-nuclei theory, even for deeply inelastic channels.

In contrast to the adiabatic-nuclei approximation, the local-complex-potential model fails severely for the $^2\Sigma_u^+$ shape resonance in H_2 . The cross sections obtained using this approximation are off by factors up to 10 and could be included in Fig. 7 only after rescaling them by appropriate factors as indicated in the figure. The cross sections obtained in the local approximation are generally much too large, in particular for dissociative attachment. The resonance peaks in the vibrational excitation functions are too high in energy and too narrow, while the width of the dissociative attachment profile is too large (see Fig. 7). The local-complex-potential model reproduces the vibrational fine structure seen in the $v=0 \rightarrow 3$

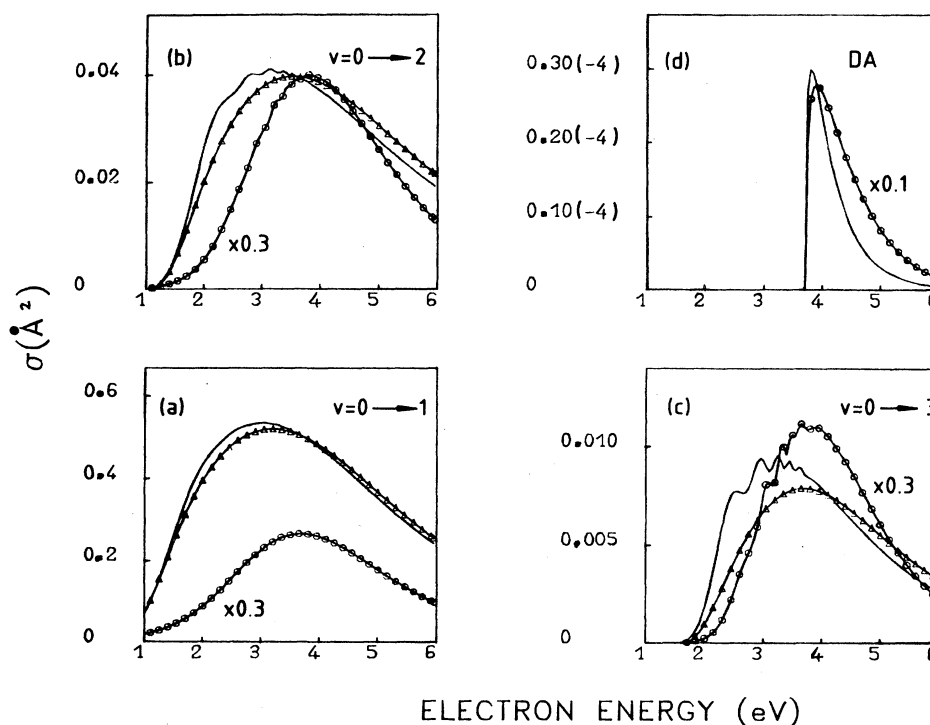


FIG. 7. Integral cross sections for vibrational excitation [(a)–(c)] and dissociative attachment (d) in H_2 calculated in the adiabatic-nuclei approximation (solid curve with triangles) and the local-complex-potential approximation (solid curve with circles) compared to the exact result (solid curve). For the purpose of display, the results of the local-complex-potential model have been scaled down by factors of 0.3 [(a)–(c)] and 0.1 (d), respectively.

and higher inelastic cross sections qualitatively, but not quantitatively, i.e., the positions and intensities of the fine-structure peaks are not identical to those found in the nonlocal calculation.

The local approximation also fails to reproduce the isotope effect in dissociative attachment and the dependence of the dissociative attachment cross section on the initial vibrational state. The local calculation yields a cross-section ratio of 90 for dissociative attachment in H_2 versus D_2 , compared to the nonlocal result of 200. The dependence of the dissociative attachment cross sections on v is less pronounced than in the nonlocal calculation and thus not in agreement with experiment (see Table II).

In recent years several variants of the local approximation have been discussed in an attempt to overcome the limitations of this model for resonances near threshold and broad resonances. The earliest proposal^{77,78} may be termed the "partly local approximation." Here only the width $\Gamma(R, E - \tilde{H}_0)$ is treated as a nonlocal operator, while the corresponding level-shift $\Delta(R, E - \tilde{H}_0)$ is approximated by a local function and can thus be included by a redefinition of the discrete-state energy. The "semilocal approximation"^{57,60} takes account of the fact that the energy dependence of the entrance and exit amplitudes is important to guarantee the correct threshold behavior of the cross sections. In this approximation the resolvent in Eq. (23) is evaluated in the local approximation, keeping the exact energy-dependent entry and exit amplitudes. Finally, Hazi *et al.*,²⁶ in their *ab initio* study of dissociative attachment in F_2 , have chosen to approximate the nonlocal level-shift operator $\Delta(R, E - \tilde{H}_0)$ by the local but still energy-dependent quantity $\Delta(R, E - \bar{\epsilon})$, where $\bar{\epsilon}$ is a suitable mean vibrational energy.

We have tested the performance of these variants of the local approximation for the present case. The partly local and semilocal models fail as badly as the standard local model. The approximation of Hazi *et al.*²⁶ yields results for vibrational excitation which are very similar to the adiabatic-nuclei theory (and thus acceptable), but gives a wrong energy dependence for the dissociative attachment cross section. We have to conclude that a completely nonlocal treatment of the nuclear dynamics in the $^2\Sigma_u^+$ resonance of H_2 is essential. In particular, the nonlocality of the level-shift operator is not negligible. The complete failure of the local approximation is a consequence of the large width of the $^2\Sigma_u^+$ resonance and its proximity to threshold.

The present *ab initio* results demonstrate most clearly that the empirical local complex potentials determined by Chen and Peacher¹⁴ and by Bardsley and Wadehra¹⁶ by fitting dissociative attachment and vibrational excitation data within the local resonance model are meaningless. This fact has already been indicated by the severe discrepancies between the potentials of Refs. 14 and 16, as pointed out by Nesbet.¹⁷ In Fig. 1 we have included the real part of the local potential and the width $\Gamma(R)$ of Bardsley and Wadehra (short-dashed lines). Both real and imaginary parts of the empirical local potential deviate strongly from the *ab initio* result at short distances, where the $^2\Sigma_u^+$ resonance is broad. This finding stresses the nonuniqueness of empirical local potentials for broad res-

onances emphasized previously.⁷⁶ Our results also have implications for the associative detachment reaction, which is the reverse process to dissociative attachment and thus given by the same T -matrix element. Associative detachment cross sections for H^-H collisions have been calculated in Refs. 20 and 21 using the local-complex-potential model, but Bieniek²² has pointed out inconsistencies in the results which indicate a breakdown of the local approximation. To obtain reliable associative detachment cross section in H^-H collisions, a nonlocal treatment appears indispensable.

IV. CONCLUSIONS

We have performed an *ab initio* study of resonant vibrational excitation and dissociative attachment in H_2 and D_2 using the projection-operator approach. The fixed-nuclei electron-molecule-scattering T matrix and eigenphase sum have been decomposed into a background term and resonant term in such a manner that the background term becomes a smooth function of energy and is weakly dependent on the internuclear distance, all rapid variations being contained in the resonant term. The fixed-nuclei resonance parameters $\epsilon_d(R)$, $\Gamma(R, E)$, and $\Delta(R, E)$ of the $^2\Sigma_u^+$ shape resonance have been calculated for a grid of energies and internuclear distances employing an accurate many-body optical potential for the $e-H_2$ interaction, as discussed in detail in I. These *ab initio* data were interpolated and extrapolated in E and R by fitting suitable analytic functions. For the resulting model, fully converged cross sections for vibrational excitation and dissociative attachment were obtained. The nuclear dynamical problem has been solved with the help of a rapidly convergent separable expansion of the nonlocal part of the effective potential for the nuclear motion in the resonance state. The contribution of the background term to inelastic and reactive processes was shown to be negligible owing to its weak dependence on the internuclear distance. Without any adjustment of the *ab initio* data we obtain cross sections which are in rather good agreement with experiment for $0 \rightarrow 1$ and $0 \rightarrow 2$ vibrational excitation and dissociative attachment. This calculation represents, in particular, the first *ab initio* treatment of dissociative attachment in H_2 .

The present study complements earlier *ab initio* calculations of vibrational excitation in N_2 via the $^2\Pi_g$ resonance^{25,34,42} and dissociative attachment via the $^2\Sigma_u^+$ resonance in F_2 ,²⁶ which are based on essentially the same formalism as used here. For the $^2\Sigma_u^+$ resonance in H_2 the strength of the nonlocal Feshbach resonance theory is particularly apparent. The local-complex-potential model fails completely, both for electron scattering and dissociative attachment. The off-shell adiabatic-nuclei approximation is found to be satisfactory for a qualitative description of vibrational excitation, but does not provide reactive cross sections such as the dissociative attachment cross section.

An interesting feature of the calculated cross sections is the appearance of fine structure in deeply inelastic vibrational excitation channels of H_2 . Although the details of this fine structure depend very sensitively on the fixed-

nuclei resonance parameters ϵ_d , Γ , and Δ , we believe that this prediction is correct in principle and that vibrational fine structure should be observable in sufficiently inelastic channels. The appearance of vibrational substructure also indicates that the vibrational close-coupling expansion may be slowly convergent for higher channels.

Considering the three above-mentioned electron-molecule-scattering resonances for which accurate calculations including the nuclear dynamics have been performed, a consistent picture concerning the validity of the local-complex-potential model begins to emerge. For the comparatively narrow ${}^2\Pi_g$ shape resonance in N_2 the local approximation is of excellent accuracy, although there are significant deviations from the nonlocal theory in the vibrationally elastic channel.²⁵ For the ${}^2\Sigma_u^+$ shape resonance in F_2 the local approximation is bound to fail, since this resonance crosses the threshold in the Franck-Condon zone and threshold effects are not properly treated in the local model.^{26,48,78} As quantitatively shown in this work, the local approximation is also inadequate for the ${}^2\Sigma_u^+$ resonance in H_2 owing to the large width of this resonance and the proximity of the threshold, which results in a strong energy dependence of the width $\Gamma(E)$ and the level-shift $\Delta(E)$. We have to conclude that the local-complex-potential model for vibrational excitation and

dissociative attachment should be applied only to comparatively narrow resonances which do not cross the threshold in the vicinity of the equilibrium geometry of the target molecule.

Forthcoming more complete and more accurate calculations of vibrational excitation and dissociative attachment in H_2 should include the rotational motion and should be based on accurate fixed-nuclei *ab initio* data which extend into the asymptotic region $R \rightarrow \infty$. The nonlocal ${}^2\Sigma_u^+$ potential employed in the present work is only of qualitative accuracy at large internuclear distances due to the analytic extrapolation of the *ab initio* data beyond $R=2.75$ a.u. A presumably very accurate potential-energy function of the ${}^2\Sigma_u^+$ bound state of H_2^- for $R \geq 3.0$ a.u. has recently been obtained by Senekowitsch *et al.*⁶⁵ These data may serve as reference values for more accurate analytic parametrizations of the Feshbach resonance parameters in the asymptotic region.

ACKNOWLEDGMENTS

This work has been supported by the Deutsche Forschungsgemeinschaft (DFG) through Sonderforschungsbereich 91.

*Present address: Fritz Haber Molecular Dynamics Research Center, The Hebrew University, 91904 Jerusalem, Israel.

¹G. J. Schulz, *Rev. Mod. Phys.* **45**, 423 (1973).

²R. N. Compton and J. N. Bardsley, in *Electron-Molecule Collisions*, edited by I. Shimamura and K. Takayanagi (Plenum, New York, 1984).

³*Electron-Molecule Scattering*, edited by S. C. Brown (Wiley, New York, 1979).

⁴H. Ehrhardt, L. Langhans, F. Linder, and H. S. Taylor, *Phys. Rev.* **173**, 222 (1968).

⁵F. Linder and H. Schmidt, *Z. Naturforsch.* **26a**, 1603 (1971).

⁶G. J. Schulz and R. K. Asundi, *Phys. Rev.* **158**, 25 (1967).

⁷J. N. Bardsley, A. Herzenberg, and F. Mandl, *Proc. Phys. Soc. London* **89**, 305 (1966).

⁸J. N. Bardsley, A. Herzenberg, and F. Mandl, *Proc. Phys. Soc. London* **89**, 321 (1966).

⁹R. J. W. Henry, *Phys. Rev. A* **2**, 1349 (1970).

¹⁰R. J. W. Henry and E. S. Chang, *Phys. Rev. A* **5**, 276 (1972).

¹¹A. Klonover and U. Kaldor, *Chem. Phys. Lett.* **51**, 321 (1977); *J. Phys. B* **11**, 1623 (1978); **12**, 323 (1979); **12** L61 (1979); **12**, 3797 (1979).

¹²M. A. Morrison, A. N. Feldt, and D. Austin, *Phys. Rev. A* **29**, 2518 (1984).

¹³M. A. Morrison, A. N. Feldt, and B. C. Saha, *Phys. Rev. A* **30**, 2811 (1984); see also N. F. Lane, in *Electronic and Atomic Collisions*, edited by J. Eichler, I. V. Hertel, and N. Stolterfoht (North-Holland, Amsterdam, 1984), p. 127.

¹⁴J. C. Y. Chen and J. L. Peacher, *Phys. Rev.* **167**, 30 (1968).

¹⁵J. M. Wadehra and J. N. Bardsley, *Phys. Rev. Lett.* **41**, 1795 (1978).

¹⁶J. N. Bardsley and J. M. Wadehra, *Phys. Rev. A* **20**, 1398 (1979); J. M. Wadehra, *ibid.* **29**, 106 (1984).

¹⁷R. K. Nesbet, *Comments At. Mol. Phys.* **11**, 25 (1981).

¹⁸I. Eliezer, H. S. Taylor, and J. K. Williams, *J. Chem. Phys.* **47**, 2165 (1967).

¹⁹C. W. McCurdy and R. C. Mowrey, *Phys. Rev. A* **25**, 2529 (1982).

²⁰J. Mizuno and J. C. Y. Chen, *Phys. Rev.* **187**, 167 (1969); *Phys. Rev. A* **4**, 1500 (1971).

²¹R. J. Bieniek and A. Dalgarno, *Astrophys. J.* **228**, 635 (1979).

²²R. J. Bieniek, *J. Phys. B* **13**, 4405 (1980).

²³G. Drukarev and S. Pozdnev, *J. Phys. B* **13**, 2611 (1980).

²⁴J. P. Gauyacq, in *Wave Functions and Mechanisms from Electron Scattering Processes*, Vol. 35 of *Lecture Notes in Chemistry*, edited by F. A. Gianturco and G. Stefani (Springer, Berlin, 1983), p. 122, and unpublished.

²⁵M. Berman, H. Estrada, L. S. Cederbaum, and W. Domcke, *Phys. Rev. A* **28**, 1363 (1983); H. Estrada, M. Berman, L. S. Cederbaum, and W. Domcke, *Chem. Phys. Lett.* **97**, 352 (1983).

²⁶A. U. Hazi, A. E. Orel, and T. N. Rescigno, *Phys. Rev. Lett.* **46**, 918 (1981).

²⁷B. I. Schneider and L. A. Collins, *J. Phys. B* **15**, L335 (1982); *Phys. Rev. A* **27**, 2847 (1983).

²⁸T. L. Gibson and M. A. Morrison, *Phys. Rev. A* **29**, 2497 (1984).

²⁹H. Feshbach, *Ann. Phys. (N.Y.)* **19**, 287 (1962).

³⁰J. C. Y. Chen, *Phys. Rev.* **148**, 66 (1966); **156**, 12 (1967).

³¹T. F. O'Malley, *Phys. Rev.* **150**, 14 (1966).

³²J. N. Bardsley, *J. Phys. B* **1**, 349 (1968); **1**, 365 (1968).

³³W. Domcke and L. S. Cederbaum, *Phys. Rev. A* **16**, 1465 (1977).

³⁴A. U. Hazi, T. N. Rescigno, and M. Kurilla, *Phys. Rev. A* **23**, 1089 (1981).

³⁵J. B. Delos and W. R. Thorson, *J. Chem. Phys.* **70**, 1774 (1979).

³⁶T. F. O'Malley, *Adv. At. Mol. Phys.* **7**, 223 (1971).

³⁷See, for example, N. F. Lane, *Rev. Mod. Phys.* **52**, 29 (1980).

³⁸A. U. Hazi, in *Electron-Molecule and Photon-Molecule Collisions*, edited by T. Rescigno, V. McKoy, and B. Schneider

- (Plenum, New York, 1979), p. 281.
- ³⁹A. U. Hazi, in *Electron-Atom and Electron-Molecule Collisions*, edited by J. Hinze (Plenum, New York, 1983), p. 103.
- ⁴⁰M. Berman and W. Domcke, *Phys. Rev. A* **29**, 2485 (1984).
- ⁴¹B. I. Schneider, M. Le Dourneuf, and P. G. Burke, *J. Phys. B* **12**, L365 (1979).
- ⁴²B. I. Schneider, M. Le Dourneuf, and V. K. Lan, *Phys. Rev. Lett.* **43**, 1926 (1979).
- ⁴³M. Berman, C. Mündel, and W. Domcke, *Phys. Rev. A* **31**, 641 (1985), henceforth referred to as I.
- ⁴⁴L. S. Cederbaum and W. Domcke, *Adv. Chem. Phys.* **36**, 205 (1977); J. Schirmer and L. S. Cederbaum, *J. Phys. B* **11**, 1889 (1978).
- ⁴⁵J. Schwinger, *Phys. Rev.* **72**, 742 (1947); B. A. Lippmann and J. Schwinger, *ibid.* **79**, 469 (1950).
- ⁴⁶D. K. Watson and V. McKoy, *Phys. Rev. A* **20**, 1474 (1979).
- ⁴⁷W. Domcke, *Phys. Rev. A* **28**, 2777 (1983).
- ⁴⁸C. Mündel and W. Domcke, *J. Phys. B* **17**, 3593 (1984).
- ⁴⁹S. K. Adhikari and I. H. Sloan, *Phys. Rev. C* **11**, 1133 (1975).
- ⁵⁰C. Lanczos, *J. Res. Natl. Bur. Stand.* **45**, 367 (1950).
- ⁵¹E. W. Knapp and D. J. Diestler, *J. Chem. Phys.* **67**, 4969 (1977); J. T. Broad, *Phys. Rev. A* **26**, 3078 (1982).
- ⁵²J. S. Bell and E. J. Squires, *Phys. Rev. Lett.* **3**, 96 (1959).
- ⁵³A. B. Migdal, *Theory of Finite Fermi Systems and Applications to Atomic Nuclei* (Wiley, New York, 1967).
- ⁵⁴R. R. Scheerbaum, C. M. Shakin, and R. M. Thaler, *Ann. Phys. (N.Y.)* **76**, 333 (1973).
- ⁵⁵M. Shugard and A. U. Hazi, *Phys. Rev. A* **12**, 1895 (1975).
- ⁵⁶E. Ficocelli Varrachio, *J. Phys. B* **14**, L511 (1981).
- ⁵⁷J. N. Bardsley, in Ref. 38, p. 267.
- ⁵⁸W. Domcke, *J. Phys. B* **14**, 4889 (1981).
- ⁵⁹D. T. Birtwistle and A. Herzenberg, *J. Phys. B* **4**, 53 (1971).
- ⁶⁰L. S. Cederbaum and W. Domcke, *J. Phys. B* **14**, 4665 (1981).
- ⁶¹W. Kolos and L. Wolniewicz, *J. Chem. Phys.* **41**, 3663 (1964); *J. Mol. Spectrosc.* **54**, 303 (1975).
- ⁶²G. Herzberg, *Molecular Spectra and Molecular Structure. I. Spectra of Diatomic Molecules*, 2nd ed. (Van Nostrand, New York, 1950).
- ⁶³F. V. Bunkin and I. I. Tugov, *Phys. Rev. A* **8**, 601 (1973).
- ⁶⁴E. P. Wigner, *Phys. Rev.* **73**, 1002 (1948).
- ⁶⁵J. Senekowitsch, P. Rosmus, W. Domcke, and H.-J. Werner, *Chem. Phys. Lett.* **111**, 211 (1984).
- ⁶⁶H. S. Taylor and F. E. Harris, *J. Chem. Phys.* **39**, 1012 (1963).
- ⁶⁷A. Dalgarno and A. E. Kingston, *Proc. Phys. Soc. London* **73**, 455 (1959).
- ⁶⁸M. Abramowitz and I. Stegun, *Handbook of Mathematical Functions* (Dover, New York, 1965).
- ⁶⁹A tabulation of the data of Ref. 4 is given in the review article by S. Trajmar, D. F. Register, and A. Chutjian [*Phys. Rep.* **97**, 219 (1983)].
- ⁷⁰A. Herzenberg and F. Mandl, *Proc. R. Soc. London, Ser A* **270**, 48 (1962).
- ⁷¹W. Domcke and L. S. Cederbaum, *J. Phys. B* **13**, 2829 (1980).
- ⁷²N. Chandra and A. Temkin, *Phys. Rev. A* **13**, 188 (1976).
- ⁷³E. S. Chang and S. F. Wong, *Phys. Rev. Lett.* **38**, 1327 (1977).
- ⁷⁴M. Allan and S. F. Wong, *Phys. Rev. Lett.* **41**, 1791 (1978).
- ⁷⁵F. H. M. Faisal and A. Temkin, *Phys. Rev. Lett.* **28**, 203 (1972).
- ⁷⁶M. Berman, L. S. Cederbaum, and W. Domcke, *J. Phys. B* **16**, 875 (1983).
- ⁷⁷F. Fiquet-Fayard, *J. Phys. B* **8**, 2880 (1975); G. Parlant and F. Fiquet-Fayard, *ibid.* **9**, 1617 (1976).
- ⁷⁸J. N. Bardsley and J. M. Wadehra, *J. Chem. Phys.* **78**, 7227 (1983).